Direct Imaging of Nanoscale Phase Separation in $La_{0.55}Ca_{0.45}MnO_3$: Relationship to Colossal Magnetoresistance

J. Tao,[1,2,*] D. Niebieskikwiat,[3,4] M. Varela,[1] W. Luo,[5,1] M. A. Schofield,[2] Y. Zhu,[2] M. B. Salamon,[3,6] J. M. Zuo,[7,8] S. T. Pantelides,[5,1] and S. J. Pennycook[1,5]

[1]*Materials Science and Technology Division, Oak Ridge National Laboratory, Oak Ridge, Tennessee 37831, USA*
[2]*Condensed Matter Physics and Materials Science Department, Brookhaven National Laboratory, Upton, New York 11973, USA*
[3]*Department of Physics, University of Illinois at Urbana-Champaign, Urbana, Illinois 61801, USA*
[4]*Colegio de Ciencias e Ingeniería, Universidad San Francisco de Quito, Quito, Ecuador*
[5]*Department of Physics and Astronomy, Vanderbilt University, Nashville, Tennessee 37235, USA*
[6]*Department of Physics, University of Texas at Dallas, Richardson, Texas 75080, USA*
[7]*The Frederick Seitz Material Research Laboratory, University of Illinois at Urbana-Champaign, Urbana, Illinois 61801, USA*
[8]*Department of Materials Science and Engineering, University of Illinois at Urbana-Champaign, Urbana, Illinois 61801, USA*

(Received 26 March 2009; published 27 August 2009)

A nanoscale phase is known to coincide with colossal magnetoresistance (CMR) in manganites, but its volume fraction is believed to be too small to affect CMR. Here we provide scanning-electron-nanodiffraction images of nanoclusters as they form and evolve with temperature in $La_{1-x}Ca_xMnO_3$, $x = 0.45$. They are not doping inhomogeneities, and their structure is that of the bulk compound at $x = 0.60$, which at low temperatures is insulating. Their volume fraction peaks at the CMR critical temperature and is estimated to be 22% at finite magnetic fields. In view of the known dependence of the nanoscale phase on magnetic fields, such a volume fraction can make a significant contribution to the CMR peak.

DOI: 10.1103/PhysRevLett.103.097202 PACS numbers: 75.47.Gk, 61.05.jm, 71.30.+h, 75.47.Lx

Doped manganites have been extensively studied for their unusual properties such as colossal magnetoresistance (CMR) [1,2]. A CMR peak generally appears near the temperature of a transition from a high-temperature insulating paramagnetic (PM) phase to a low-temperature conducting ferromagnetic (FM) phase, leading to suggestions that it arises from spin alignment in a percolation path of FM islands [3]. Recently, both experiments and theory led to the realization that nanoscale phase separation underlies the insulating-metal transition and is the key to understanding the high-field MR effect of the type that produces CMR in these materials [4,5]. Evidence for the nanoscale phase has been provided by diffraction techniques. It was found that the PM-FM phase transitions in CMR manganites often entail a fairly wide temperature range in which not only the PM and FM phases coexist, but a third ''CO'' phase [6,7], which is the ground state at other doping levels [1,2], is also present [8–11]. This third CO phase is characterized by unique superlattice reflections with a correlation length of a few nanometers and has attracted particular attention because it forms in the same temperature range as CMR [8,10]. These data are hard to quantify, however. In particular, it has not been definitively established whether the short range CO phase is a fluctuation in an otherwise homogeneous sample [12] or it exists in the form of clusters, which would be the signature of nanoscale phase separation [9,10]. Furthermore, the role of the nanoscale CO phase in the formation of the CMR peak has not been established experimentally. On the contrary, available estimates of the volume fraction of the CO phase [smaller than 0.1% in $La_{0.75}(Ca_{0.45}Sr_{0.55})_{0.25}MnO_3$ [10] or at most a few percent in $La_{0.67}Ca_{0.33}MnO_3$ [9]] have been viewed as far too small to account for a major role in the CMR phenomenon [10]. These volume-fraction estimates, however, are highly uncertain because they are derived from diffraction data without direct observation of the nanoscale CO phase [9,10] and its spatial distribution.

In this Letter, we use an experimental structural probe with nanometer resolution, namely, scanning electron nanodiffraction (SEND), to study mixed-phase regions in the phase diagram of one of the most widely studied systems, $La_{1-x}Ca_xMnO_3$ (LCMO), at doping level $x = 0.45$ [13]. According to the known LCMO phase diagram [1], at $x = 0.45$ the ground state is FM, becoming PM at high temperatures, while for $x \geq 0.5$ the ground state is CO. LCMO at $x = 0.45$ exhibits a CMR effect around the PM-FM transition temperature. Our technique gives direct images of a nanoscale CO phase as it evolves through the PM-FM transition region and permits determination of its volume fraction. We find that the CO-phase volume fraction is maximum at precisely the same temperature as the CMR reaches its peak and is large enough (22% at finite fields within the electron microscope) to account for a significant fraction of the total CMR peak over a background magnetoresistance that is caused by conventional spin alignment mechanisms [3]. We also provide evidence that the CO nanoscale phase is not caused by chemical inhomogeneities and discuss other possible origins.

The experiments were performed on single-crystal domains of polycrystalline LCMO prepared by the nitrate decomposition route [14]. Results obtained from different single-crystal domains are similar, and representative re-

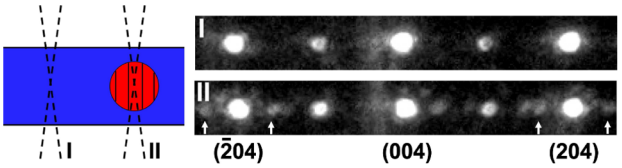

FIG. 1 (color online). Left: A schematic showing the principle of the SEND. Right: END patterns at the [010] zone of *Pnma* $La_{0.55}Ca_{0.45}MnO_3$ for the beam located off and on a CO cluster, shown as position I (no SLRs) and II (SLRs marked by the arrows), respectively.

sults are shown in this Letter. Figure 1 shows the principle of SEND and the interpretation of the data. The electron beam in a transmission electron microscope (TEM) is focused down to a probe size ~1.7 nm with a convergent angle of less than 1 mrad and scanned over the sample in a single-crystal domain. The small convergent angle is achieved on a JEOL 2010F TEM using a 4 μm condenser aperture. At every point, an electron nanodiffraction (END) pattern is acquired. Only when the electron beam is located on the CO phase do superlattice reflections (SLRs) corresponding to the ordered structure appear. The measured intensities of the SLRs allow us to map the real space distribution of the CO phase. The local superlattice wave vector q_{CO}/a^* is determined to be 0.40 from the recorded END patterns from this material, which is the same as that of the long range CO phase that exists at low temperatures in bulk materials at $x = 0.60$ [15]. This result is consistent with previous publications [8–10] with the added feature that our diffraction data are obtained from individual nanodomains. Figure 2 shows images obtained in this way as the temperature is increased through the FM-PM phase transition in the $La_{0.55}Ca_{0.45}MnO_3$ sample. From the intensity images, cluster diameters are around 3–4 nm with a certain size distribution that is possibly affected by the size of the electron beam, the scanning step, and the noise on the END patterns. The CO nanoclusters' size is in agreement with previous estimates based on the widths of diffraction spots [8–10], which suggests that there is no significant electron beam effect on the size distribution of the CO nanoclusters. The SEND maps, however, definitively establish that the CO phase is present as static nanoclusters in this material. As can be directly seen from the images, the density of CO clusters peaks at a temperature of ~253 K.

Resistivity measurements of the $La_{0.55}Ca_{0.45}MnO_3$ sample under multiple magnetic fields are shown in Fig. 3(a). The CMR effect is clearly shown with a peak at $T \sim 253$ K in Fig. 3(b). The volume fraction of the CO nanoclusters is determined using the intensity maps shown in Fig. 2 and the thickness of the samples obtained by the simulations (see auxiliary material [16]). The volume fractions are plotted in Fig. 3(b) to compare with the magnetoresistance.

Figure 3(b) clearly demonstrates that the density of CO nanoclusters peaks at $T \sim 253$ K, in coincidence with the maximum CMR effect. In order to explore the role of the nanoclusters in the appearance of the CMR peak, we first note that the magnetization curve of LCMO at $x = 0.45$ shown as the inset in Fig. 3(b) shows that the system is dominated by the FM phase below $T \sim 230$ K. Therefore the background magnetoresistance below $T \sim 230$ K, whose presence is consistent with observations in other systems [4], can be accounted for by conventional mechanisms in terms of spin alignment [3]. We will now make the case that the nanoclusters play an important role in the formation of the CMR peak.

First we estimate the volume fraction of the nanoclusters as follows. We determined the thickness of the sample using convergent beam electron diffraction (CBED), which is known as a highly accurate technique for local thickness measurement. A CBED pattern was recorded in the same area as the SEND images. The experimental CBED pattern was compared with simulations based on the known crystal structure of $La_{0.5}Ca_{0.5}MnO_3$ (see auxiliary material [16]). We obtained 8 ± 1.5 nm. Given this thickness, we counted the number of the CO nanoclusters from the SEND maps in the scanning areas and estimated the volume fraction of the CO nanoclusters to be $22 \pm 7\%$ at the peak value inside our microscope (see auxiliary material [16] for details). In estimating the error bar we included the uncertainty in the thickness, in the nanocluster radius, and in the nanocluster count.

The key result is that the volume fraction is quite large, compared with previous inferences from indirect data. The volume fraction of $22 \pm 7\%$ exists in the presence of a 2.8 T magnetic field within the electron microscope, caused by the objective lens [17]. Experimental data in Ref. [11] on $Nd_{0.7}Sr_{0.3}MnO_3$ have shown that the intensity of the CO SLR decreases by a factor of 2 when the magnetic field increases from 0 to 2.8 T. Assuming that

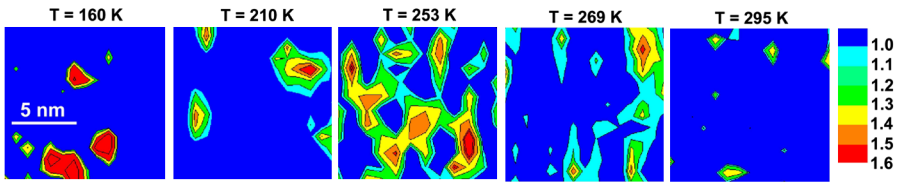

FIG. 2 (color online). Intensity maps of the superlattice reflections in $La_{0.55}Ca_{0.45}MnO_3$ as the temperature is raised through the FM-PM phase transitions. A color scale of relative intensity is shown on the right. The flat blue area has the intensity of SLRs below the noise level. Each map is from an area of 12×12 nm^2 with the scanning step of 1 nm in a single crystal domain, although each image is not necessarily in precise registration with any other.

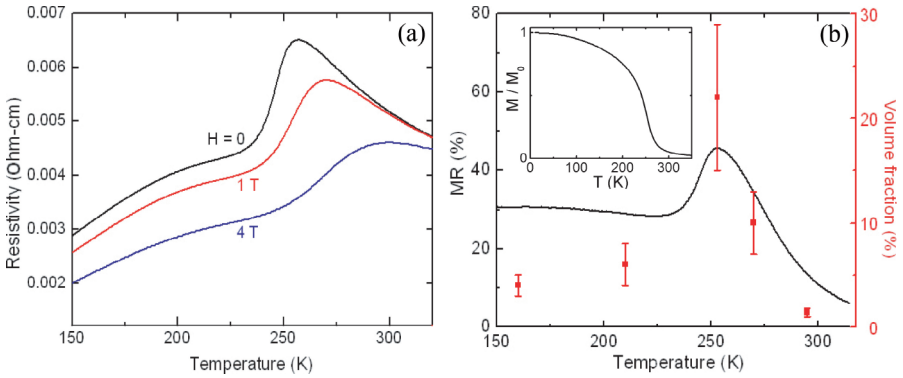

FIG. 3 (color online). (a) Resistivity versus temperature of the $La_{0.55}Ca_{0.45}MnO_3$ sample are measured under different magnetic fields $H = 0$, 1, and 4 T. (b) The magnetoresistance $[\rho(0) - \rho(4T)]/\rho(0)$ is plotted (black line) and compared with the volume fraction of the CO nanoclusters (red squares) estimated using the SEND maps shown in Fig. 2. In the inset, we show the magnetization as a function of temperature under a magnetic field of 1 T.

the nanoclusters in our samples exhibit a similar variation with the magnetic field, we conclude that the volume fraction at zero magnetic field is much larger than 22%, whereas at 4 T the volume fraction is smaller than 22%. We finally note that the CO nanoclusters are likely to be much more resistive than PM clusters because at doping levels $x > 0.5$, during the PM-to-CO transition, the material becomes monotonically more resistive [1]. The net conclusion is that at $x = 0.45$, during the PM-to-FM transition, in the neighborhood of ~253 K, the appearance of the CO nanoscale phase adds significant additional resistivity that is sensitive to magnetic fields and can be a major contributor to the CMR peak superposed on the background magnetoresistance. The most likely origin of this background magnetoresistance is spin alignment [3], as the CO nanoclusters have a very small volume fraction at temperatures below $T \sim 230$ K and thus do not affect the magnetoresistance of the system.

We turn now to explore the possible physical mechanism for the formation of the structurally distinct CO nanoclusters at large volume fractions. First, we rule out the possibility that they are merely chemical inhomogeneities by a histogram distribution of the wave vector (q_{CO}/a^*) measured in individual nanoclusters shown in Fig. 4(a) [18,19]. They are clearly centered about $q_{CO}/a^* = 0.40$, or $x_{eff} = 0.60$, where x_{eff} is defined by $x_{eff} = 1 - q_{CO}/a^*$. This specific relationship between x_{eff} and q_{CO} was established in LCMO compounds at doping levels $x \geq 0.5$, where the CO phase is most stable and becomes the ground state at low temperatures [15]. If the nanoclusters were a manifestation of chemical inhomogeneities, the distribution of the chemical concentration should be centered on the bulk average doping level $x = 0.45$ and the SLRs should come from all of the nanoclusters with local doping $x_{eff} \geq 0.5$; i.e., there would be more CO nanoclusters with $x_{eff} = 0.50$ than with $x_{eff} = 0.60$, which is clearly not the case. This conclusion is further confirmed by the images of the CO clusters at $T = 255$ K in the $La_{0.55}Ca_{0.45}MnO_3$ sample through thermal cycling, as shown in Figs. 4(b) and 4(c). With the help of alignment marks at the sample edge, the second image was obtained from the same area as the first image after warming up to and then cooling from $T = 350$ K, a temperature that is high enough to melt most CO clusters but chemical dopants are still unlikely to move. The two images show only a small amount of correlation of cluster sites and shapes [20], which shows that there is no local pinning of the CO nanoclusters, ruling out the possibility of local chemical inhomogeneity as the cause of the wave vector mismatch.

The question of why the nanoclusters in LCMO at $x = 0.45$ exhibit a structural order with $q_{CO}/a^* = 0.40$, which is the same as the structure observed in LCMO at $x = 0.60$ at low temperatures, is difficult to answer definitively. A mismatch of the q_{CO}/a^* has been reported to arise from multiple sources. One is the effect of external strain on the long range CO superstructure [21]; in our case, the q_{CO}/a^* value is constant from different crystal domains with different strains. Thus we can exclude an external-strain effect as the cause of the mismatch. The other possibility is the effective x_{eff}. Since we showed that x_{eff} is not the result of chemical disorder, it may be the result of electron transfer. In such a case, the nanoclusters would have an electron density that corresponds to $x = 0.60$, which would result in an extra positive charge of $\pm 0.15e$ per Mn site in the CO nanoclusters in $La_{0.55}Ca_{0.45}MnO_3$. Although such a

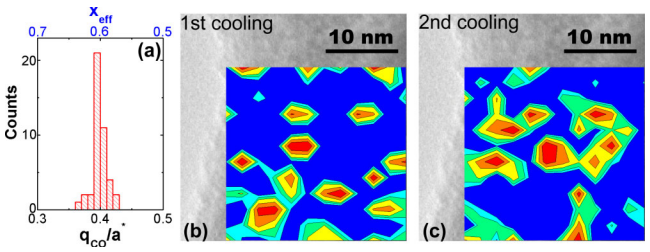

FIG. 4 (color online). (a) Distribution of CO wave vectors q_{CO}/a^* from individual nanoclusters observed from the $La_{0.55}Ca_{0.45}MnO_3$ sample at $T = 253$ K. The distribution is centered at an effective doping $x_{eff} = 1 - q_{CO}/a^*$ (plotted as the top axis) which equals 0.60. (b),(c) The intensity maps of the CO SLRs obtained using SEND at $T = 255$ K. Both maps were obtained at the same temperature and from the same area in the $La_{0.55}Ca_{0.45}MnO_3$ sample, but the map in (c) was recorded after a thermal cycle where the sample was warmed up to 350 K and cooled down again. The color scale is the same as that in Fig. 2. The backgrounds are bright field TEM images showing the same features at the sample edge which help to locate the scanning area.

transfer would entail costly Coulomb energies, it has been shown that in nanoscale clusters the electronic energy gain due to phase coexistence may stabilize the charge segregation [22,23]. Also, it may be possible that the reduced phonon energies, i.e., the elastic energy gain by the long-wavelength distortions, can balance the Coulomb energy. However, neither our structural SEND results nor available theoretical results have linked the CO superstructure in the nanoclusters to nanoscale charge segregation directly at finite temperature. Alternatively, the CO superlattice observed in the nanoclusters may simply reflect the pertinent distortions that occur in a CO phase at $x = 0.45$, and the similarity with those at $x = 0.60$ is coincidental. Finally, we note that all mechanisms that have been proposed so far for the CMR phenomenon, including the theoretical simulations that find nanoscale CO-phase separation [23], rely heavily on the assumption that the PM-FM phase transition is governed by magnetic effects. The existence of a structural nanoscale phase during the transition in the LCMO system points to the possibility that structural entropies compete with magnetic entropies. This possibility is consistent with the simulations that find a CO nanoscale phase only if coupling to lattice modes is included [23]. On the other hand, the formation of the CO nanoclusters introduces significant surface areas between the nanoclusters and the matrix. Consequently, there is a considerable surface energy that competes with the volume free energies and may play an important role in determining the size of the CO nanoclusters.

In summary, our SEND results demonstrate with nanoscale resolution that nanoclusters with dimensions ~3–4 nm in diameter evolve concomitantly with the PM-FM transition region in $La_{0.55}Ca_{0.45}MnO_3$. The volume fraction of the nanoclusters peaks at the CMR temperature and is large enough to contribute significantly to the CMR peak in terms of reduced conducting volume. The data establish that the nanoclusters are not chemical-doping inhomogeneities. The scanning electron probe technique developed opens a door to the exploration of nanoscale phase separation and its correlation to physical properties in other complex materials.

We thank Dr. R. D. Twesten and J. G. Wen for instrument support and Professor E. Dagotto, Dr. J. A. Fernandez-Baca, Dr. F. Ye, and Dr. N. D. Mathur for discussions. Research was sponsored by the Office of Basic Energy Sciences, Division of Materials Sciences and Engineering and by appointment to the ORNL Postdoctoral Research Program administered jointly by ORNL and ORISE. Work at BNL was supported by the U.S. DOE/BES under Contract No. DE-AC02-98CH10886. Support was also provided by the McMinn Endowment at Vanderbilt University. Electron diffraction was carried out at the Center for Microanalysis of Materials, the Frederick Seitz Materials Research Laboratory Central Facilities, University of Illinois, which are partially supported by the U.S. DOE under Grants No. DE-FG02-07ER46453 and No. DE-FG02-07ER46471.

*jtao@bnl.gov

[1] P. Schiffer *et al.*, Phys. Rev. Lett. **75**, 3336 (1995).
[2] M. B. Salamon and M. Jaime, Rev. Mod. Phys. **73**, 583 (2001); E. Dagotto, Science **309**, 257 (2005); C. Israel, M. J. Calderon, and N. D. Mathur, Mater. Today **10**, 24 (2007).
[3] M. Fäth *et al.*, Science **285**, 1540 (1999); M. Uehara *et al.*, Nature (London) **399**, 560 (1999); L. Zhang *et al.*, Science **298**, 805 (2002).
[4] J. M. De Teresa *et al.*, Nature (London) **386**, 256 (1997).
[5] J. A. Fernandez-Baca *et al.*, Phys. Rev. Lett. **80**, 4012 (1998); M. B. Salamon, P. Lin, and S. H. Chun, *ibid.* **88**, 197203 (2002); T. Becker *et al.*, *ibid.* **89**, 237203 (2002); J. M. De Teresa *et al.*, Phys. Rev. B **65**, 100403 (R) (2002).
[6] We retain the term "CO phase" even though experiments and theory have now established that there is no ordering of physical charge [7].
[7] W. Luo *et al.*, Phys. Rev. Lett. **99**, 036402 (2007).
[8] P. Dai *et al.*, Phys. Rev. Lett. **85**, 2553 (2000); C. P. Adams *et al.*, *ibid.* **85**, 3954 (2000).
[9] J. M. Zuo and J. Tao, Phys. Rev. B **63**, 060407(R) (2001).
[10] V. Kiryukhin *et al.*, Phys. Rev. B **67**, 064421 (2003).
[11] T. Y. Koo *et al.*, Phys. Rev. B **64**, 220405(R) (2001).
[12] R. Mathieu *et al.*, Phys. Rev. Lett. **93**, 227202 (2004); Y. Motome, N. Furukawa, and N. Nagaosa, *ibid.* **91**, 167204 (2003).
[13] The sample at doping level $x = 0.45$ was selected because its transport property measurement has a strong CMR effect and its proximity to the FM-AFM phase boundary (at $x = 0.50$) gives the CO SLR relatively high intensities.
[14] D. Niebieskikwiat *et al.*, Phys. Rev. B **66**, 134422 (2002).
[15] C. H. Chen, S.-W. Cheong, and H. Y. Hwang, J. Appl. Phys. **81**, 4326 (1997); J. C. Loudon *et al.*, Phys. Rev. Lett. **94**, 097202 (2005).
[16] See EPAPS Document No. E-PRLTAO-103-013937 for auxiliary material detailing two steps to estimate the volume fraction of the charge ordering (CO) nanoclusters. For more information on EPAPS, see http://www.aip.org/pubservs/epaps.html.
[17] V. V. Volkov *et al.*, Rev. Sci. Instrum. **73**, 2298 (2002).
[18] The deviation of the measured wave vector q_{CO}/a^* from its mean value 0.40 is mainly due to the measurement error and possibly the variations in the orientation of the CO structure [19].
[19] J. C. Loudon *et al.*, Philos. Mag. **85**, 999 (2005); D. Sanchez *et al.*, Phys. Rev. B **77**, 092411 (2008).
[20] Most of the clusters in the two maps are not correlated, while about 30% of the clusters overlap if the maps are divided into grids of about the cluster size. Calculation shows that the probability of putting the clusters with the amount shown in our maps into the same grid squares twice is about 30%, which is consistent with the experimental results.
[21] S. Cox *et al.*, Phys. Rev. B **73**, 132401 (2006).
[22] J. Lorenzana, C. Castellani, and C. Di Castro, Phys. Rev. B **64**, 235128 (2001); C. Ortix, J. Lorenzana, and C. Di Castro, *ibid.* **73**, 245117 (2006).
[23] C. Şen, G. Alvarez, and E. Dagotto, Phys. Rev. Lett. **98**, 127202 (2007); C. Şen *et al.*, Phys. Rev. B **73**, 224441 (2006).